Available online at www.sciencedirect.com
ScienceDirect
Journal of Molecular Catalysis A: Chemical 284 (2008) 155–160
JOURNAL OF MOLECULAR CATALYSIS A: CHEMICAL
www.elsevier.com/locate/molcata

The structural, physical and photocatalytic properties of the mesoporous Cr-doped TiO_2

Xiaoxing Fan [a,b], Xinyi Chen [a,c], Shaopeng Zhu [b], Zhaosheng Li [a,b,c], Tao Yu [a,c], Jinhua Ye [d], Zhigang Zou [a,c,*]

[a] *Eco-materials and Renewable Energy Research Center (ERERC), Department of Physics, Nanjing University, Nanjing 210093, People's Republic of China*
[b] *Department of Materials Science and Engineering, Nanjing University, Nanjing 210093, People's Republic of China*
[c] *National Laboratory of Solid State Microstructures, Nanjing University, Nanjing 210093, People's Republic of China*
[d] *Photocatalytic Materials Center (PCMC), National Institute for Materials Science (NIMS), 1-2-1 Sengen, Tsukuba, Ibaraki 305-0047, Japan*

Received 26 December 2006; received in revised form 26 November 2007; accepted 6 January 2008
Available online 12 January 2008

Abstract

A visible-light-active mesoporous Cr-doped TiO_2 photocatalyst with worm-like channels was synthesized using an evaporation-induced self-assembly approach and characterized by X-ray powder diffraction, nitrogen adsorption–desorption, X-ray photoelectron spectroscopy, transmission electron microscope, and UV–vis diffuse reflectance, respectively. The effect of Cr^{3+} doping concentration on the photocatalytic activity of mesoporous TiO_2 was investigated from 0.1 to 1 mol%. The characterizations indicated that the photocatalysts possessed a homogeneous pore diameter of about 8 nm with high surface area of 117 m^2/g and a crystalline anatase pore wall doped by Cr^{3+}. Compared with pure mesoporous TiO_2, the Cr-doped TiO_2 extended the photoabsorption edge into the visible light region. The results of gaseous acetaldehyde photodecomposition showed that mesoporous Cr-doped TiO_2 exhibited higher photocatalytic activities than pure mesoporous TiO_2 and nonporous Cr-doped TiO_2 under visible light irradiation.

Keywords: Cr-doped; Mesoporous TiO_2; Photocatalysis; Acetaldehyde; Photodecomposition

1. Introduction

More recently, the metal-oxide photocatalysts have become a focus of attention due to their possible application to degradation of environmental organic pollutants and the conversion of solar-energy [1–6]. Among the very few photochemically and chemically stable photocatalysts, TiO_2 (P25) is one of the most popular photocatalysts due to its high photocatalytic activity when irradiated by UV light ($\lambda < 400$ nm) [7]. It has also been clarified that the photocatalytic activity of TiO_2 strongly depends on its physical properties, such as crystal structure, surface area, particle size, surface hydroxyls, etc. [8,9]. Of these physical properties, surface area is one of the key factors in enhancing the photocatalytic activity. The larger the surface area is, the more the photocatalytic active sites are, thus enhancing the photocatalytic activity. Mesoporous TiO_2, which displayed better photocatalytic activity than P25 because of its larger surface area, has therefore received much interest in photocatalysis [10–13]. However, pure mesoporous TiO_2 only strongly absorb UV light (rather than visible light), which only accounts for a small fraction of the solar spectrum (<4%). The development of visible light responsive mesoporous TiO_2 has the positive effect on improving the photocatalytic efficiency. In addition, for practical application to decompose indoor organic pollutants, it is necessary to extend the photoabsorption of TiO_2 into visible light region. Thus, exploring visible light absorption, large surface areas and crystalline pore wall mesoporous TiO_2 is significant.

Thus for, extensive researches have been conducted to convert the TiO_2 absorption from the ultraviolet to the visible light region by the ion doping of transition metals [14]. Among these transition metal ions, Cr^{3+} has received much attention because its

* Corresponding author at: Eco-materials and Renewable Energy Research Center (ERERC), Department of Physics, Nanjing University, 22 Hankou Road, Nanjing 210093, People's Republic of China. Tel.: +86 25 83686630; fax: +86 25 8368 6632.
E-mail address: zgzou@nju.edu.cn (Z. Zou).

1381-1169/$ – see front matter © 2008 Elsevier B.V. All rights reserved.
doi:10.1016/j.molcata.2008.01.005

introduction can excellently extend the visible light absorption. In 2002, Palmisano et al. studied the photocatalytic degradation of aliphatic and aromatic compounds in aqueous systems on Cr-doped polycrystalline TiO_2 powder [15]. Afterwards, Gonzalez-Elipe et al. investigated the photocatalytic properties of Cr-doped TiO_2 thin film prepared by ion beam-induced CVD [16]. Zhang et al. studied the photooxidation of XRG (azoic dye) aqueous solution on Cr-doped TiO_2 prepared by a process that combined sol–gel with hydrothermal method. The results showed that Cr-doped TiO_2 effectively improved the photocatalytic activity under visible light irradiation within the optimal doping concentration from 0.15 to 0.2% [17]. Yin et al. synthesized the mesoporous Cr-doped TiO_2 and studied its electrorheological activity [18]. More recently, Yu et al. fabricated mesoporous Cr-TiO_2 photocatalyst and evaluated its activity for photodegradation of methylene blue. The results showed that the photocatalytic activity of mesoporous Cr-doped TiO_2 was higher than that of pure mesoporous TiO_2 [19]. However, so far, there is no systematic study on the effect of the Cr/Ti molar ratio on the acetaldehyde photodecomposition over mesoporous Cr-doped TiO_2 under visible light irradiation.

In present work, mesoporous Cr-doped TiO_2 with worm-like channels was synthesized using an evaporation-induced self-assembly approach. The effect of Cr doping concentration on the photocatalytic activity of mesoporous TiO_2 was investigated from 0.1 to 1 mol%. The photocatalytic decomposition of acetaldehyde over these obtained samples was conducted under UV-light and visible light irradiation.

2. Experimental

2.1. Preparation of catalysts

In a typical synthesis, 0.01 mol of titanium chloride ($TiCl_4$) was added to a solution containing 1 g of pluronic P123 ($EO_{20}PO_{70}EO_{20}$, $M = 5800$, Aldrich) and 10 g of ethanol. To this solution, 1×10^{-5}, 5×10^{-5} and 1×10^{-4} mol $Cr(NO_3)_3$ was added for the synthesis of mesoporous Cr-doped TiO_2, respectively. The resulting sol was gelled in an open petri dish at 50 °C in air for 4 days. The as-made bulk samples were then calcined at 400 °C for 3 h in air at the heating rate of 1 °C min^{-1} to remove the surfactant. The calcined samples were labeled according to the Cr-doping content (the pure mesoporous TiO_2 is denoted as MT-0, the mesoporous Cr-doped TiO_2 is denoted as MT-0.1 and so on). The synthesis of the nonporous 0.1 mol% Cr-doped TiO_2 labeled as Cr-TiO_2-0.1 was similarly conducted but without the surfactant of P123.

2.2. Structural characterization

Wide-angle X-ray powder diffraction (XRD) measurements were performed on a Rigaku Ultima III X-ray diffractometer using Cu Kα radiation. Nitrogen adsorption–desorption isotherms were collected on a Micromeritics Tristar-3000 surface area and porosity analyzer at 77 K after the samples had been degassed in the flows of N_2 at 150 °C for 5 h. The Brunauer–Emmet–Teller (BET) surface area was calculated from the linear part of the BET plot ($P/P_0 = 0.1$–0.25). The pore size distribution plots were obtained by using the Barret–Joyner–Halenda (BJH) model. Images of high-resolution transmission electron microscope (HRTEM) were obtained by employing a TECNAI F20 high-resolution transmission electron microscope with a 200 kV accelerating voltage. The X-ray photoelectron spectroscopy (XPS) measurements were carried out on an ESCALAB Mark II (VG Company, U.K.). The UV–vis diffuse reflectance spectrum was measured on a UV–vis spectrophotometer (UV-2550, Shimadzu).

2.3. Investigations of photocatalytic properties

The photocatalytic activities of the prepared samples for the oxidation of acetaldehyde in air were examined at room temperature. In a typical process, powder sample (0.1 g) was put on a 4-cm^2 glass groove. The glass with powder photocatalyst was then placed into a 224-ml gastight reactor with a quartz window, filled with air to one atmospheric pressure. Then, acetaldehyde (5 μl of 40% CH_3CHO aqueous solution) was injected into the reactor to generate a high-concentration acetaldehyde gas. The light source for the catalytic reaction was a 300-W Xe arc lamp. The evolved carbon dioxide was detected by a Shimadzu GC-14B gas chromatograph equipped with a methanizer and a FID detector.

3. Results and discussion

3.1. Powder X-ray diffraction analysis

Fig. 1 shows the wide-angle XRD patterns of the samples calcined at 400 °C. Only the single anatase TiO_2 (JCPDS, No. 21-1272) was formed and no chromium oxide impurity phase was detected. Similar results have been reported previously [17]. In fact, Cr^{3+} ions can be easily incorporated into the TiO_2 lattice via displacing Ti^{4+} sites due to their close ionic radius of Ti^{4+} (0.68 Å) and Cr^{3+} (0.64 Å) [20]. In addition, the mean crystalline sizes calculated by the Scherrer equation are summarized in

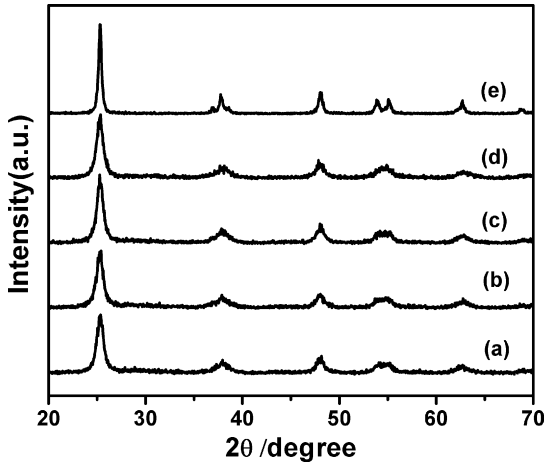

Fig. 1. Wide-angle XRD patterns of mesoporous Cr-doped TiO_2 sample with different Cr^{3+} content: MT-0 (a), MT-0.1 (b), MT-0.5 (c), MT-1 (d) and Cr-TiO_2-0.1 (e).

Table 1
Summary of the physicochemical properties of mesoporous Cr-doped TiO_2

Samples	Crystal size (nm)	Surface area (m^2/g)	D-BJH (nm)	V-total (cm^3/g)
MT-0	9.2 (0.2)	101.0	5.2	0.180
MT-0.1	8.8 (0.2)	117.8	7.8	0.332
MT-0.5	9.4 (0.2)	116.0	7.6	0.314
MT-1	9.1 (0.2)	114.2	8.0	0.324
Cr-TiO_2-0.1 (non-pore)	19.6 (0.1)	49.6	–	–

Table 1. All the mean crystalline sizes are about 9.0 nm. This phenomenon could be ascribed to the lower doping content that is not large enough to affect the growth of anatase crystals.

3.2. Nitrogen physisorption and TEM characterization

The pore size distributions and N_2 adsorption–desorption isotherms of pure mesoporous TiO_2 and MT-0.1 are shown in Fig. 2. Both the isotherms reveal stepwise adsorption and desorption, which is a characteristic of mesoporous materials. The narrow pore size distribution curves indicated that the present materials have uniform pore channels. The narrow pore size distribution is not affected by the doped concentration of Cr^{3+} even when the Cr^{3+} content of the precursors is as high as 1 mol%. The BET surface areas of these samples with different Cr-doping contents are also listed in Table 1. It can be seen that Cr-doped TiO_2 samples have about 10% larger BET surface areas than pure mesoporous TiO_2.

Transmission electron microscopy observations were performed to confirm the mesostructure existence in the TiO_2. A wormhole-like mesostructure without long-range order was observed on the edges of Cr-doped mesoporous TiO_2, as shown in Fig. 3. As indicated by HRTEM images, anatase nanocrystals are clearly observed to connect with each other to form crystalline framework walls of the mesopore.

3.3. XPS studies

The X-ray photoelectron spectra of mesoporous Cr-doped TiO_2 are shown in Fig. 4. The typical full XPS spectra (Fig. 4A) of mesoporous Cr-doped TiO_2 showed that the mesoporous Cr-doped TiO_2 contains only Ti, O, Cr and a trace amount of carbon, indicating chloride ion and the template are removed via calcination. The peaks at 458.05 and 463.75 eV (see Fig. 4B) are indexed to Ti^{4+} $2p_{3/2}$ and Ti^{4+} $2p_{1/2}$, respectively. The Ti 2p peaks are in quite close good agreement with that of pure TiO_2. The peaks of XPS spectra of Cr 2p (see Fig. 4C) at 576.05 and 588.05 eV should be assigned to Cr^{3+} $2p_{3/2}$ and Cr^{3+} $2p_{1/2}$, respectively [19–21]. Therefore, in the mesoporous Cr-doped TiO_2, the valence states of Ti and Cr ions are +4 and +3, respectively.

3.4. Photocatalytic performance

Fig. 5 shows the UV–vis absorption spectra of mesoporous Cr-doped TiO_2. It is obvious that the doped Cr^{3+} can significantly improve the absorption of mesoporous TiO_2 in the visible light region. The absorption at wavelength of less than 387 nm is caused by the intrinsic band gap absorption of anatase TiO_2 (3.2 eV). The absorption around 450 nm is due to the charge transfer band $Cr^{3+} \rightarrow Ti^{4+}$ or $^4A_{2g} \rightarrow {}^4T_{1g}$ of Cr^{3+} in an octahedral environment, and, the broad absorption band from 620 to 800 nm is due to $^4A_{2g} \rightarrow {}^4T_{2g}$ d–d transitions of Cr^{3+} [17,21]. With the increase in Cr^{3+} doping content, the absorption edge of mesoporous TiO_2 greatly extended into the visible light region. This extended absorbance indicates the possible enhancement in the photocatalytic activity of mesoporous TiO_2 illuminate by visible light.

The photocatalytic activity for acetaldehyde photodecomposition was evaluated by the amount of evolved carbon dioxide in the reaction. The overall process of acetaldehyde photodecomposition over TiO_2 can be depicted by the following equation

$$2CH_3CHO + 5O_2 \xrightarrow{TiO_2, h\nu} 4CO_2 + 4H_2O \quad (1)$$

To confirm that degradation of acetaldehyde over Cr-doped mesoporous TiO_2 proceeds photocatalytically, a parallel comparisons experiment was carried out over SiO_2 powders. SiO_2

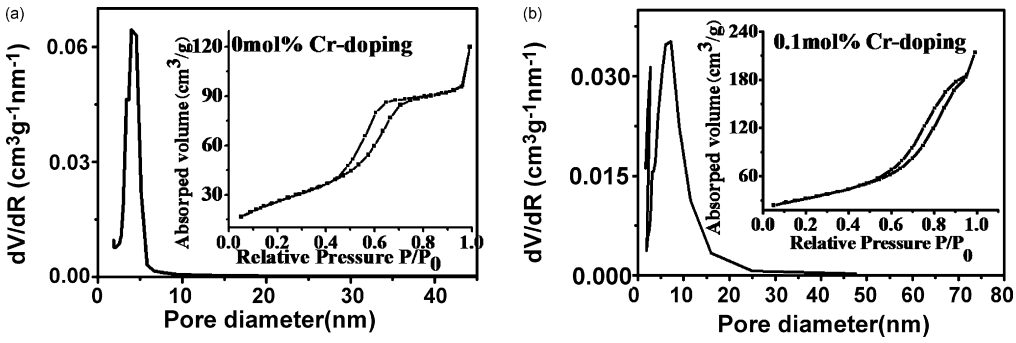

Fig. 2. N_2 adsorption–desorption isotherms and Barret–Joyner–Halenda (BJH) pore size distribution (inset) of (a) MT-0 and (b) MT-0.1.

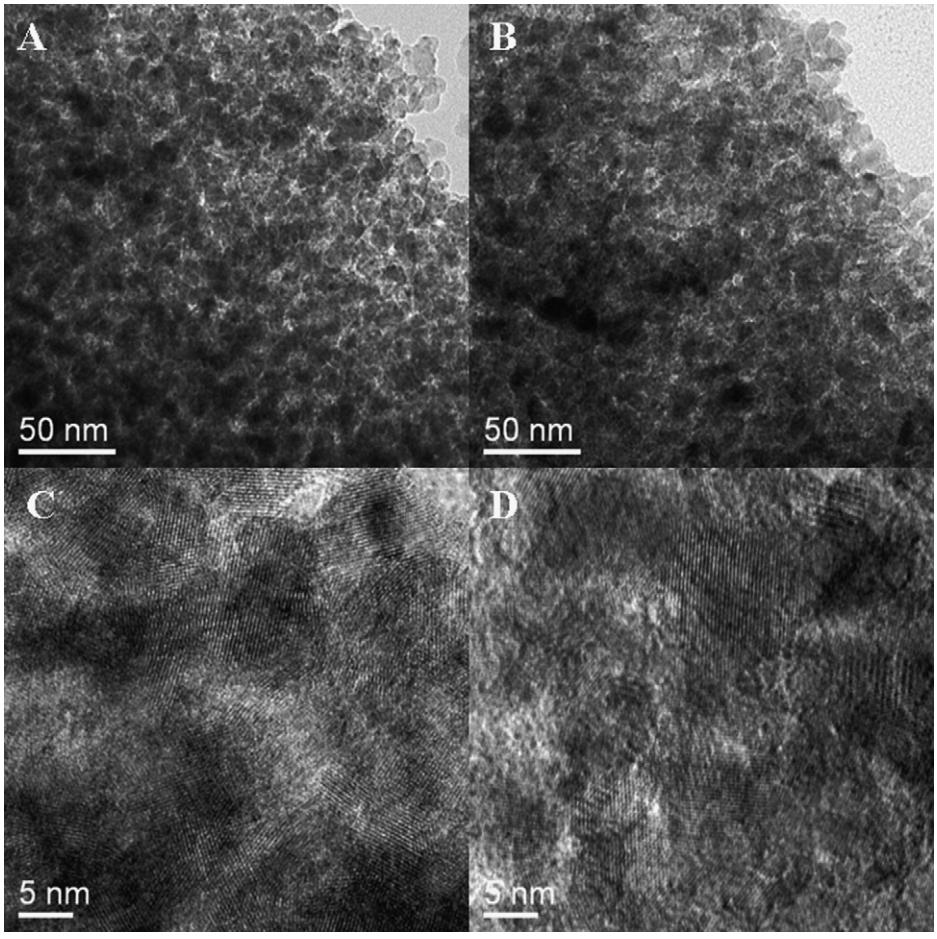

Fig. 3. TEM and HRTEM images of MT-0.1(A and C) and MT-1(B and D).

powders (0.1 g) was placed into the photocatalytic reactor and tested under the same conditions. No obvious increase in amount of CO_2 was detected. Additionally, MT-0.1 sample was tested under ($\lambda > 440$ nm) visible light irradiation without acetaldehyde injection. After 3 h photoreaction, the amount of increased evolved dioxide was 0.0531 μmol, which only accounts for 0.3% of the produced carbon dioxide (17.9 μmol) in acetaldehyde photodecomposition reaction. Therefore, the evolved carbon dioxide (99.7% of total) mainly comes from the photodecomposition of acetaldehyde in the photoreaction. The evolved carbon dioxide in the blank experiment may be coming from the adsorbed carbon dioxide on the sample.

Fig. 6 shows the amount of carbon dioxide produced from the photocatalytic degradation of acetaldehyde on MT-0, MT-0.1,

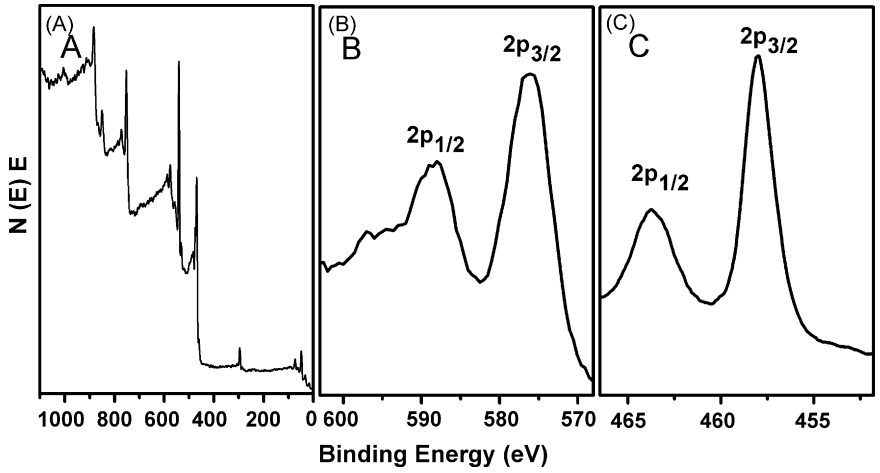

Fig. 4. XPS spectra of calcined mesoporous Cr-doped TiO_2 (A), Cr2p XPS spectra (B) and Ti2p spectra (C) of MT-0.1.

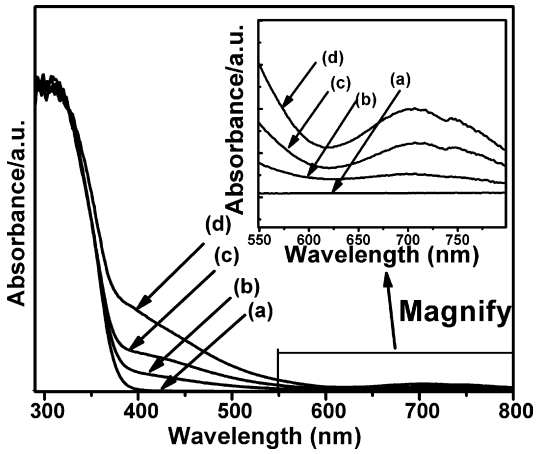

Fig. 5. UV–vis diffuse reflectance spectra of mesoporous Cr-doped TiO_2 samples: MT-0 (a), MT-0.1 (b), MT-0.5 (c) and MT-1 (d).

MT-0.5, MT-1, Cr-TiO_2-0.1, and P25 under UV light irradiation (full arc of Xe lamp). MT-0 exhibited a higher photocatalytic activity than P25, which can be attributed to its mesoporous structure that provides more active sites for the reaction. The introduction of Cr^{3+} into the mesoporous framework decreased the photocatalytic activity of mesoporous TiO_2. Moreover, with the increase in the Cr content in mesoporous TiO_2, the photocatalytic activity gradually decreased. This result can be attributed to the formation of crystal defects (oxygen vacancy) caused by Cr^{3+} substitution for Ti^{4+} in the TiO_2 lattice, which act as recombination centers for the photogenerated electrons and holes. The more defects as well as the higher Cr^{3+} concentration will lead to lower photocatalytic activity.

Although Cr^{3+} doping leads to the formation of defects, it can enhance the activity of mesoporous TiO_2 under visible light. Fig. 7 shows the amount of evolved carbon dioxide on different samples irradiated under visible light at wavelength $\lambda > 440$ nm. In comparison with the photocatalytic activity with UV-light irradiation, the MT-0.1 rather than MT-0 exhibited the highest activity. This result should be due to the positive effect of Cr^{3+} introduction on the photocatalytic activity because the Cr-doping not only increases the surface area of mesoporous TiO_2 but also extends its photoabsorption to visible light region. It was found that the photocatalytic activity of P25 was much lower than that of other samples because P25 only can utilize ultraviolet light. Though the surface area of Cr-TiO_2-0.1 is 50% of that of MT-0.1, the photocatalytic activity was comparable with that of MT-0.1. This phenomenon should be attributed to the higher crystallinity of Cr-TiO_2-0.1 than that of MT-0.1. The higher the crystalline quality is, the smaller the amount of defects is, as the defects usually act as trapping and recombination centers for photogenerated electrons and holes, thus resulting in the decrease in the photocatalytic activity [22]. The MT-0 catalyst exhibited a similar high activity to the mesoporous Cr-doped TiO_2 samples under visible light irradiation. This could be caused by the remaining carbon doped into the TiO_2. Previous researches have reported that the photocatalytic reaction can proceed on C-doped TiO_2 under visible light irradiation [23,24]. However, the amount of carbon impurity in Cr-doped mesoporous TiO_2 is less and its function is limited. From the UV–vis absorption spectra of samples, it can be seen that the intensity and region of visible light photoabsorption on mesoporous Cr-doped TiO_2 is stronger and larger, respectively than those of MT-0. The strong absorption is beneficial to the photocatalytic activity because the available photons are proportional to photoabsorption. So, if the reaction is carried out under visible light with longer wavelength than 440 nm, mesoporous Cr-doped TiO_2 should exhibit higher photocatalytic activity than MT-0. The amount of evolved carbon dioxide on photocatalysts under visible light irradiation ($\lambda > 460$ nm) is shown in Fig. 8. As expected, the photocatalytic activity of MT-0.1 is twice higher than that of MT-0, indicating the doped Cr^{3+} plays a dominant role in enhancing photocatalytic activity under visible light irradiation.

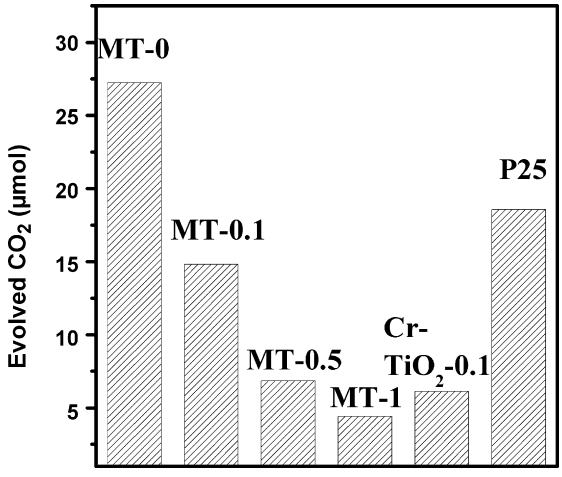

Fig. 6. The photocatalytic activities of samples under UV-light (full arc of 300 W Xe lamp). The reaction was carried out for 15 min.

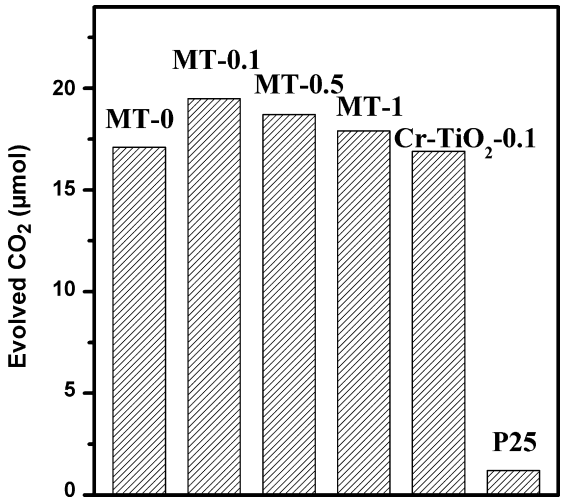

Fig. 7. The photocatalytic activities of samples under visible light irradiation ($\lambda > 440$ nm). The reaction was carried out for 3 h.

As well known, one common problem in semiconductor photocatalysis is that the photoreactions have many critical variables such as surface area, defects concentration and photoabsorption. The surface area is one of the key factors to control the photocatalytic activity of a photocatalyst. The larger the surface area is, the higher the photocatalytic activity is. In addition, the con-

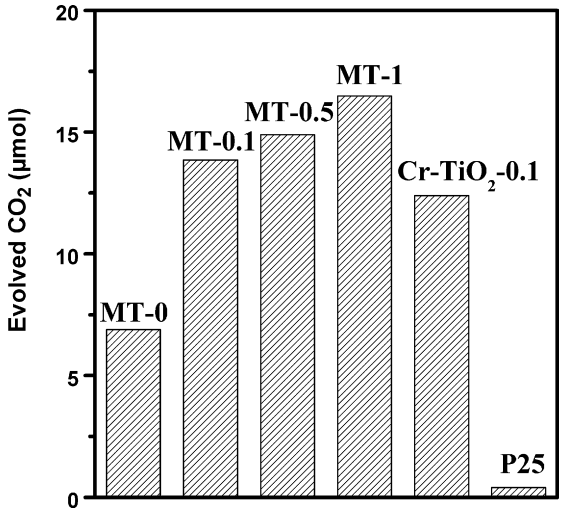

Fig. 8. The photocatalytic activities of samples under visible light irradiation ($\lambda > 460$ nm). The reaction was carried out for 3 h.

centration of defects caused by ion doping and/or by the poor crystallinity influences the activity significantly, because such defects will act as recombination centers for photogenerated electrons and holes, thus decreasing the photocatalytic activity. Furthermore, the photoabsorption characters greatly affect the photocatalytic activity of a photocatalyst, since the numbers of absorbed photons directly depend on the absorption property of the photocatalyst. In our experiment, the amount of doped Cr^{3+} affects the photocatalytic activity of mesoporous Cr-doped TiO_2. For example, MT-0.1 exhibits the highest photocatalytic activity under visible light irradiation ($\lambda > 440$ nm), while MT-1 is the best when irradiated by light above 460 nm. This phenomenon could be explained by the competition and balance of the three factors above.

4. Conclusions

Mesoporous Cr-doped TiO_2 materials have been synthesized by using the evaporation-induced self-assembly method. Cr^{3+} doping can significantly improve the photoabsorption and slightly increase the surface area of mesoporous TiO_2. In gaseous acetaldehyde photodecomposition, the doped Cr^{3+} improved the photocatalytic activity of mesoporous TiO_2 under visible light irradiation especially under $\lambda > 460$ nm. The factors such as surface area, defects concentration and photoabsorption affect the photocatalytic activity of mesoporous Cr-doped TiO_2.

Acknowledgments

Financial support from the National Natural Science Foundation of China (Nos. 20603017 and 20528302), the National High Technology Research and Development Program of China (No. 2006AA05Z113), the Science and Technology Research Program of the Ministry of Education (MOE) of China (No.307012) and the National Basic Research Program of China (973 Program, 2007CB613301, 2007CB613305) is gratefully acknowledged. This work was also supported by the Scientific Research Foundation of Graduate School of Nanjing University (2006CL05). Prof. Z.G. Zou and T. Yu would like to thank the Jiangsu Provincial Talent Scholars Program.

References

[1] A. Fujishima, K. Honda, Nature 238 (1972) 37–38.
[2] A. Mills, S.L. Hunte, J. Photochem. Photobiol. A 108 (1997) 1–35.
[3] D.A. Tryk, A. Fujishima, K. Honda, Electrochim. Acta 45 (2000) 2363–2376.
[4] M.R. Hoffmann, S.T. Martin, W. Choi, D.W. Bahnemann, Chem. Rev. 95 (1995) 69–96.
[5] Z. Zou, J. Ye, K. Sayama, H. Arakawa, Nature 414 (2001) 625–627.
[6] A. Hagfeldt, M. Grätzel, Acc. Chem. Res. 33 (2000) 269–277.
[7] T. Kawahara, Y. Konishi, H. Tada, N. Tohge, J. Nishii, S. Ito, Angew. Chem. Int. Ed. 41 (2002) 2811–2813.
[8] B. Ohtani, Y. Ogawa, S. Nishimoto, J. Phys. Chem. B 101 (1997) 3746–3752.
[9] N. Serpone, A.V. Emeline, Res. Chem. Intermed. 31 (2005) 391–432.
[10] D.M. Antonelli, J.Y. Ying, Angew. Chem. Int. Ed. Engl. 34 (1995) 2014–2017.
[11] J.Y. Ying, AIChE J. 46 (2000) 1902–1906.
[12] J.C. Yu, L. Zhang, Z. Zheng, J. Zhao, Chem. Mater. 15 (2003) 2280–2286.
[13] J.C. Yu, X. Wang, X. Fu, Chem. Mater. 16 (2004) 1523–1530.
[14] S. Karvinen, Solid State Sci. 5 (2003) 811–819.
[15] A.D. Paola, E. García-López, S. Ikeda, G. Marcì, B. Ohtani, L. Palmisano, Catal. Today 75 (2002) 87–93.
[16] F. Cracia, J.P. Holgado, A. Caballero, A.R. Gonzalez-Elipe, J. Phys. Chem. B 108 (2004) 17466–17476.
[17] J. Zhu, Z. Deng, F. Chen, J. Zhang, H. Chen, M. Anpo, J. Huang, L. Zhang, Appl. Catal. B: Environ. 62 (2006) 329–335.
[18] J.B. Yin, X.P. Zhao, J. Phys. Chem. B 110 (2006) 12916–12925.
[19] J.C. Yu, G.S. Li, X.C. Wang, X.L. Hu, C.W. Leung, Z.D. Zhang, Chem. Commun. 25 (2006) 2717–2719.
[20] J.B. Yin, X.P. Zhao, Chem. Mater. 16 (2004) 321–328.
[21] H. Kato, A. Kudo, J. Phys. Chem. B 106 (2002) 5029–5034.
[22] A. Kudo, H. Kato, I. Tsuji, Chem. Lett. 33 (2004) 1534–1539.
[23] Y. Choi, T. Umebayashi, M. Yoshikawa, J. Mater. Sci. 39 (2004) 1837–1839.
[24] W.J. Ren, Z.H. Ai, F.L. Jia, L.Z. Zhang, X.X. Fan, Z.G. Zou, Appl. Catal. B: Environ. 69 (2007) 138–144.